ELSEVIER

Carbohydrate Research 292 (1996) 129–141

CARBOHYDRATE
RESEARCH

The complex of amylose and iodine

Xiaochun Yu [a,*], Carl Houtman [a], Rajai H. Atalla [a,b]

[a] *Chemical Engineering Department, University of Wisconsin–Madison, Madison, WI 53706, USA*
[b] *USDA, Forest Products Laboratory, One Gifford Pinchot Dr., Madison, WI 53705-2398, USA*

Received 22 January 1996; accepted 22 May 1996

Abstract

The organization of polyiodide chains in the amylose–iodine complex was investigated by Raman spectroscopy, by UV/vis, and by second-derivative UV/vis spectroscopies complemented by semiempirical calculations based on a simple structural model. The Raman spectra indicate that the primary substructures of the polyiodide chains are I_3^- and I_5^- sub-units. The second derivatives of the UV/vis spectra reveal four absorption peaks that can be attributed to the four polyiodide species I_9^{3-}, I_{11}^{3-}, I_{13}^{3-}, and I_{15}^{3-} on the basis of AM1 calculations and a polyiodide structural model. In an amylose–iodine–iodide solution, the polyiodides within the amylose helices exist in equilibrium with iodine and iodide. Changing the iodide concentration causes changes in the relative population of the different polyiodide chains and their substructures. The change in population of the various polyiodide species is accompanied by a corresponding shift in the positions of the UV/vis absorption maxima. The Raman spectra reflect parallel changes in the population of the I_3^- and I_5^- subunits. The proposed polyiodide chain lengths are consistent with previously reported observations concerning changes in the color characteristics of iodine–amylose complexes with the length of the amylose molecule up to a dp between 40 and 50. © 1996 Elsevier Science Ltd.

Keywords: Amylose; Polyiodide; Pentaiodide; Triiodide; Iodide; Iodine

1. Introduction

For many decades now, solutions of iodine and iodides have been used as stains to facilitate identification of cellulosic fibers. A number of different formulations have been used, but they all rely on the differential staining of cell-wall polysaccharides for their function. For example, Graff 'C' stain gives colors that range from red to yellow to blue depending on the origin of the fibers and the treatments used in their isolation [1]. The molecular origin of this differential staining is poorly understood. In order to

---

[*] Corresponding author.

PII S0008-6215(96)00159-0

establish a basis for a broader examination of the mechanism of color formation in iodine–polysaccharide complexes, we have re-examined the iodine–amylose system, since its solution structure is relatively well understood. Specifically, we seek a better understanding of the organization of the molecular complex responsible for the color.

The deep-blue complex that amylose forms with iodine is well known [2]. The structure of the complex has been established by Rundle et al. [3–8], who, on the basis of X-ray diffraction studies, concluded that the amylose is organized as left-handed helices, which have outer diameters of 13 Å and a pitch of 8 Å, with each turn of the helix corresponding to six 1,4-anhydroglucose units. The iodine components appear to be linearly arranged in the 5 Å wide inner cavity of the helices with an I–I distance of approximately 3.1 Å. Although it is widely accepted that the iodine-derived species in the macromolecular helix from a polyiodide chain is responsible for the blue color, some questions about the organization of the polyiodide entities remain. These questions occur with respect to the length of the polyiodide chains, the substructures within these chains, the charges associated with the substructures, as well as the precursors under different conditions of preparation.

Some attempts at estimating the polyiodide chain length have been made. In 1953 Ono et al. [9], using Kuhn's equation for polyenes [10], concluded that the polyiodide chain contains 40–160 iodine atoms, depending on iodide concentration, and that these chains are responsible for the absorption in the UV/vis spectrum with a λ_{max} between 588 and 620 nm. This calculation reflected the polyiodide chain-length dependence on the iodide concentration, but since this calculation relies on an estimate of the polyiodide chain length at zero iodide concentration, its accuracy is uncertain. Furthermore, the chain length proposed is inconsistent with the experimental observation that amylose with a dp of 40–50 can form a blue complex [11,12]. If the molecular model proposed by Rundle et al. [3–8] for the iodine–starch complex is correct, an amylose chain of 40 glucose units would accommodate no more than 17 iodine atoms. Thus the estimate of Ono et al. [9] appears to be at least 2–8 times too large. Using potentiometric titration at low iodide concentrations, Gilbert and Marriot [13] concluded that the I_2/I^- ratio of the polyiodide is approximately 3/2, and thus the polyiodide responsible for the blue color has the empirical formula $(I_8)^{2-}$. They cannot exclude, however, other species of polyiodide or polyiodide mixtures that will give the same I_2/I^- ratio. Many other chain lengths have been proposed, namely, $(I_7)^-$ and $(I_9)^-$ [14], $(I_6)^{2-}$, $(I_8)^{2-}$, and $(I_{10})^{2-}$ [15], I_4^{2-} [16], I_6 [17], and I_{24}^{2-} [18]. In addition, the theoretical calculations of Cramer and Herbst [19] indicated that the polyiodide exhibiting a λ_{max} at 620 nm contains about 14–15 iodine atoms. Thus, although there have been many studies addressing the question of polyiodide chain length, a conclusive resolution has heretofore remained elusive.

Another controversial question about the starch–iodine complex is the nature and charge of the polyiodide substructures. The earliest hypothesis was that the cavity of the starch helix is nonpolar and, thus, serves as a nonpolar solvent. The I_2 molecules then dissolve in the hydrophobic interior as discrete units as shown in structure (**A**) [20,21].

—I-I—I-I—I-I—I-I—I-I—I-I—I-I—I-I—

A

A recent report by Minick et al. [17] advocates this structure and presents the general formula for the complex as $(C_6H_{10}O_5)_{16.5}I_6$. But this structure is not consistent with some of the other experimental data: (1) potentiometric titration [13] indicated the necessity of I^- for the complex formation; (2) the I_2/I^- ratio in the complex varies with iodide concentration [13]; (3) the Raman spectra of the colored complex exclude the presence of discrete iodine molecules [22]; (4) the UV/vis spectra [23] point to the necessity of iodide for the formation of a blue complex and for the shift in the absorption maximum with changing iodide concentration.

It is now generally accepted that iodide plays an important role in the formation of the starch–iodine complex. The structure of (benzamide)$_2H^+I_3^-$ has led some investigators to propose a model based on I_3^- as the discrete units, as in structure (**B**) [24–26].

$$\text{—}I\text{-}\bar{I}\text{-}I\text{—}I\text{-}\bar{I}\text{-}I\text{—}I\text{-}\bar{I}\text{-}I\text{—}I\text{-}\bar{I}\text{-}I\text{—}I\text{-}\bar{I}\text{-}I\text{—}I\text{-}\bar{I}\text{-}I\text{—}I\text{-}\bar{I}\text{-}I\text{—}$$

B

But this structural model is also not consistent with the Raman spectra obtained for (benzamide)$_2H^+I_3^-$ [22]. Furthermore, it represents an I_2/I^- ratio equal to 1 and is independent of iodide concentration. This model does not fit the experimental observation by Gilbert and Marriot [13] that at an iodide concentration of 10^{-4} M, the I_2/I^- ratio is about 3/2, and that the I_2/I^- ratio depends on iodide concentration. The X-ray diffractometric investigation of model compounds by Noltemeyer and Saenger [27] suggests that the exclusive occurrence of either of the single species I_2 or I_3^-, as in structures **A** and **B**, can be safely eliminated.

Teitelbaum et al. [22] proposed yet another structure model **C** based on similarities between the Raman and Mössbauer spectra of the starch–iodine complex and those of polycrystalline (trimesic acid · $H_2O)_{10}H^+I_5^-$.

$$\text{—}I\text{-}I\text{-}\bar{I}\text{-}I\text{-}I\text{—}I\text{-}I\text{-}\bar{I}\text{-}I\text{-}I\text{—}I\text{-}I\text{-}\bar{I}\text{-}I\text{-}I\text{—}I\text{-}I\text{-}\bar{I}\text{-}I\text{-}I\text{—}I\text{-}I\text{-}\bar{I}\text{-}I\text{-}I\text{—}I\text{-}I\text{-}\bar{I}\text{-}I\text{-}I\text{—}$$

C

Although this structure model has received acceptance, it remains inconsistent with some of the experimental observations mentioned earlier, and it does not resolve some of the questions raised. As with the two previous models discussed, structure **C** represents an I_2/I^- ratio that is inconsistent with the results of the potentiometric titration experiments and the observation that this ratio depends on iodide concentration [13]. Furthermore, the assignment of Raman spectra, which is the primary basis for Teitelbaum's proposal, is at variance with other reports on these spectra. Four principal peaks at 27, 55, 109, and 160 cm^{-1} have been observed in the Raman spectra of starch–iodine complexes [15,22,28,29]. These were assigned by Teitelbaum to I_5^- because they match the spectrum of the model compound polycrystalline (trimesic acid · $H_2O)_{10}H^+I_5^-$, but the assignment of 109 cm^{-1} to I_5^- is questionable. In fact, this peak has been widely assigned to the symmetric stretching vibration of I_3^- [30–34]. The Raman spectra of polycrystalline (trimesic acid · $H_2O)_{10}H^+I_5^-$ has also been thoroughly investigated by Nour et al. [32]. Based on their theoretical calculations and far-infrared data, they assigned the peak at 109 cm^{-1} to the presence of I_3^- impurity and not to I_5^-.

Mizuno and Tanaka [34] have even used the relative intensities of the peaks at 160 and 109 cm^{-1} to estimate the I_5^- to I_3^- ratio. The assignment of 109 cm^{-1} to I_5^- is also inconsistent with the changes in relative intensities of the other peaks. The height of the 109 cm^{-1} peak relative to the other peaks increases with increasing iodide concentration [15]. This is confirmed by observations in the present work to be described in following sections. Thus, the peak at 109 cm^{-1} is ascribed to the I_3^- symmetric stretching vibration, and it is likely that Teitelbaum's starch–iodine complex samples were exhibiting bands of both I_3^- and I_5^-.

In reviewing the results summarized above, it is clear that some significant questions remain concerning the nature of starch–iodine complexes. In particular, it seems clear that the possibility that I_3^- and I_5^- coexist in the complexes needs to be considered. Their relationship within the polyiodide chain that is responsible for the characteristic blue color remains uncertain. In the present work, the polyiodide chains in amylose–iodine complexes were investigated through an orchestrated examination of the Raman, UV/vis, and second-derivative UV/vis spectra, together with semiempirical calculations of the collective electronic energy levels of the chains. Together, these methods can provide complementary information about both the substructures that exist within the complexes and the collective electronic transitions that are responsible for the gradation of their colors when the conditions of preparation are varied.

2. Results

FT Raman spectra of amylose–iodine complexes.—The Raman spectra of amylose–iodine complexes formed under different conditions are shown in Fig. 1. The spectra are similar to the previously published results in the region above 60 cm^{-1}, which shows two fundamental peaks at 110 and 160 cm^{-1}. The spectra in Fig. 1, however, do not show bands at 25 and 50 cm^{-1}, which are likely to be attenuated by the Rayleigh line filter in the FT Raman spectrometer system. For the purposes of the present study, observation of the two major bands near 110 and 160 cm^{-1} is quite adequate.

The relative intensities of the two peaks near 110 and 160 cm^{-1} change with iodide concentration. A complex formed in a high concentration iodide solution exhibits an intense peak at 160 cm^{-1} and a smaller peak at 110 cm^{-1}. As the iodide concentration is decreased, the intensity of the peak at 110 cm^{-1}, relative to the one at 160 cm^{-1}, declines significantly; the complex formed in a saturated iodine solution, without added iodide, exhibits only a shoulder at 110 cm^{-1}. These results clearly support the interpretation assigning the two bands to different chemical species, for otherwise their relative intensities would remain constant. Furthermore, we found that the intensity change is reversible. Increasing the ratio of iodide concentration to that of iodine enhances the peak at 110 cm^{-1}, while reducing the ratio results in a reduction in the peak height. This indicates a dynamic equilibrium between the polyiodide chains and iodine and iodide. It is interesting that, over a wide range of iodine and iodide concentrations, the peak at 160 cm^{-1} is always the most intense. This may, in part, be due to the I_5^- possessing a higher scattering coefficient than I_3^-, since it has more π electrons and its electronic absorption bands extend further into the visible range. Given that the relative concentration of I_3^- to I_5^- cannot be determined independently, it

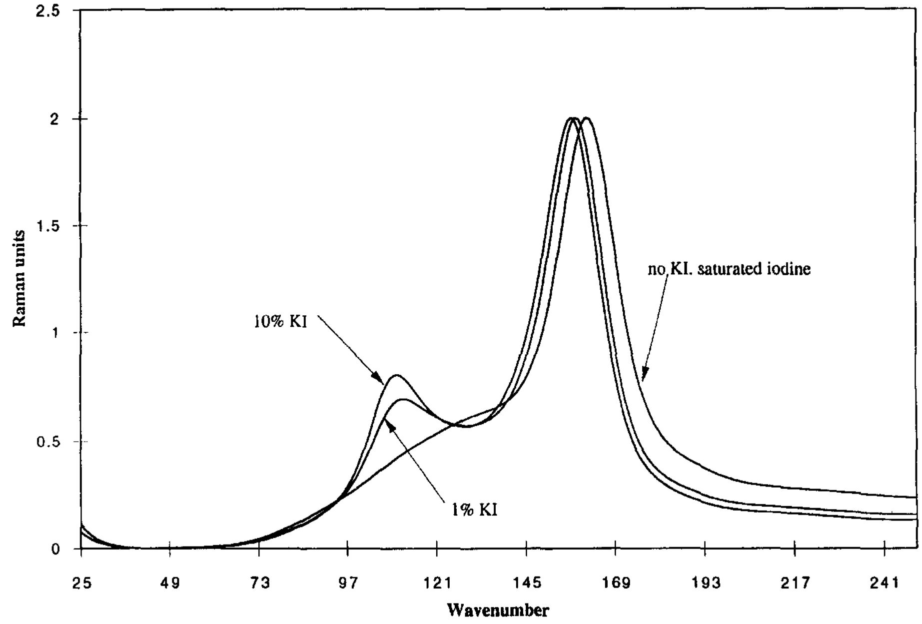

Fig. 1. Raman spectra of amylose–iodine complexes formed from solutions that are saturated in I_2 and have the indicated concentration of KI.

appears that only part of the I_5^- can be converted into I_3^-, while a residual amount of the I_5^- remains unaffected.

In addition to changing the relative intensities of the bands, changes in the iodide and iodine concentration also shift the position of the peak near 160 cm^{-1}. When the amylose–iodine complex is formed from the a saturated iodine solution without added iodide, the peak appears at 165 cm^{-1}. With increasing iodide concentration, the peak shifts to lower wavenumber; when the complex is formed in a solution with 10% iodide, the peak appears at 157 cm^{-1}. Clearly, an increase in the negative charge density of the polyiodide structure within the complex results in a shift of this peak to lower frequencies.

The Raman spectra of samples isolated by freeze-drying were also investigated. Examples of these spectra are shown in Fig. 2. It is observed that after a relatively short treatment, the peak intensity of 110 cm^{-1} increases in comparison to the spectrum of the saturated solution. This effect is quite likely the result of dissociation of I_5^- to I_3^- and I_2, with the I_2 subliming into the vapor phase. When the sample is treated under freeze-drying conditions for 10 h, a point is reached where further treatment under the same condition does not result in any significant change. This suggests that the level of I_5^- achieves a stable level beyond which further dissociation is very limited. Murdoch [35] has studied the iodine loss by gravimetric methods. He noted that the weight change due to iodine loss also can be divided two stages. The first stage is much faster than the second one. This experimental observation is consistent with the changes observed in the Raman spectra upon freeze-drying.

Freeze-drying also influences the peak positions; the peak near 160 cm^{-1} shifts to a lower wavenumber. When the complex is formed from saturated iodine solution, the position is 165 cm^{-1}, but after freeze-drying this peak shifts to 160 cm^{-1}. As explained above, this may reflect an increase of negative charge density in the polyiodide chain.

In summary, the Raman spectral data point to the likelihood that I_5^- and I_3^- are the key substructures of the longer polyiodide chains, and that, under conditions which favor dissociation of the I_5^- units, some of them dissociate, with the I_2 subliming and leaving I_3^- in the polyiodide chain. These data are consistent with an equilibrium model, which is illustrated below. It assumes that a linear array of the substructures is stabilized by the amylose helix, with the balance between the population of the substructures determined by the conditions of preparation and other post-isolation treatments.

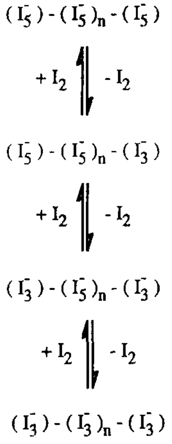

Equilibrium I

UV/vis spectral analysis of the amylose–iodine complex.—The UV/vis spectra of the amylose–iodine complexes prepared with different iodide concentrations are shown in Fig. 3. As has been widely reported, the amylose–iodine complex exhibits a broad and asymmetric absorption peak, with its maximum near 600 nm and a shoulder at about 480 nm. When the iodide concentration is increased, the absorption maximum shifts to shorter wavelengths.

Since the adsorption spectrum appears to be composed of several overlapping peaks which are difficult to resolve, the second derivatives of these spectra [36,37] were analyzed. With second-derivative spectra, the positions of maximum negative curvature correspond to peaks in the original spectra. The second derivatives of the absorption spectra are shown in Fig. 4.

The second-derivative spectra indicate that, at low iodide concentration, the UV/vis spectra consist of four peaks with their the maxima near 460–480 nm, 560–590 nm, 660–700 nm, and 710–740 nm; their exact positions are difficult to pinpoint. At higher

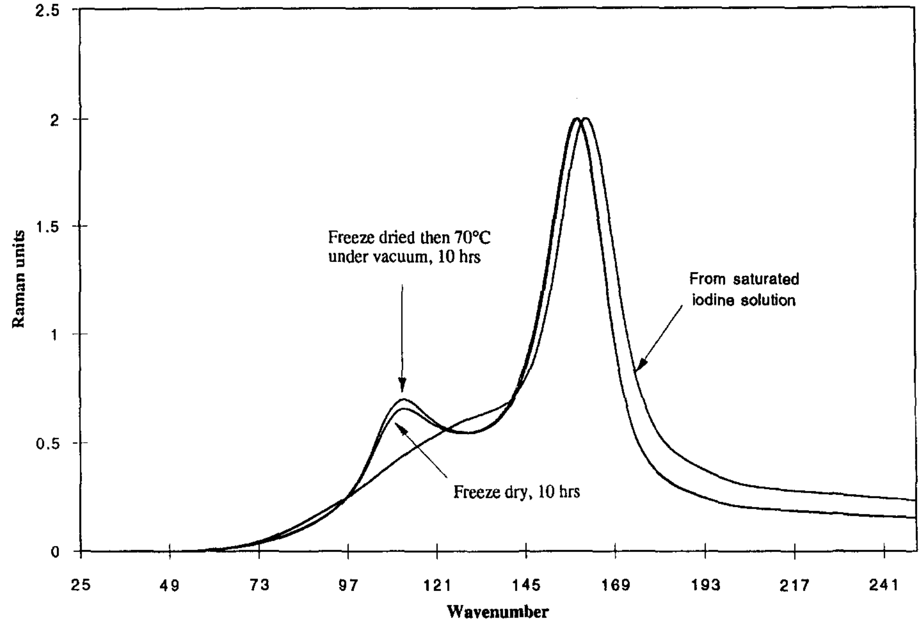

Fig. 2. Raman spectra of amylose–iodine complexes after various treatments. The spectrum labelled 'saturated solution' was obtained before the sample was freeze-dried.

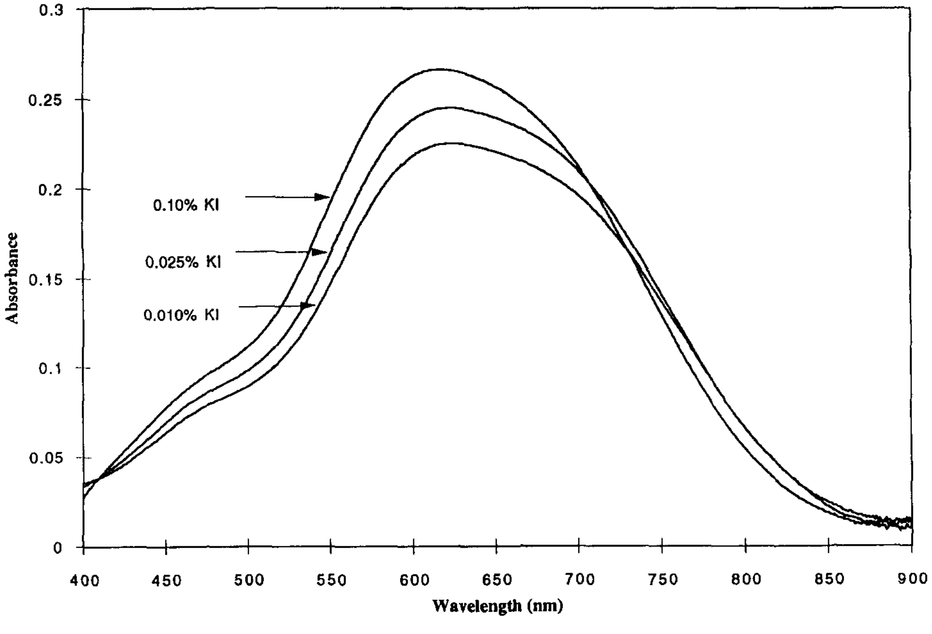

Fig. 3. UV spectra of amylose–iodine complexes formed from solutions that have the indicated concentration of KI.

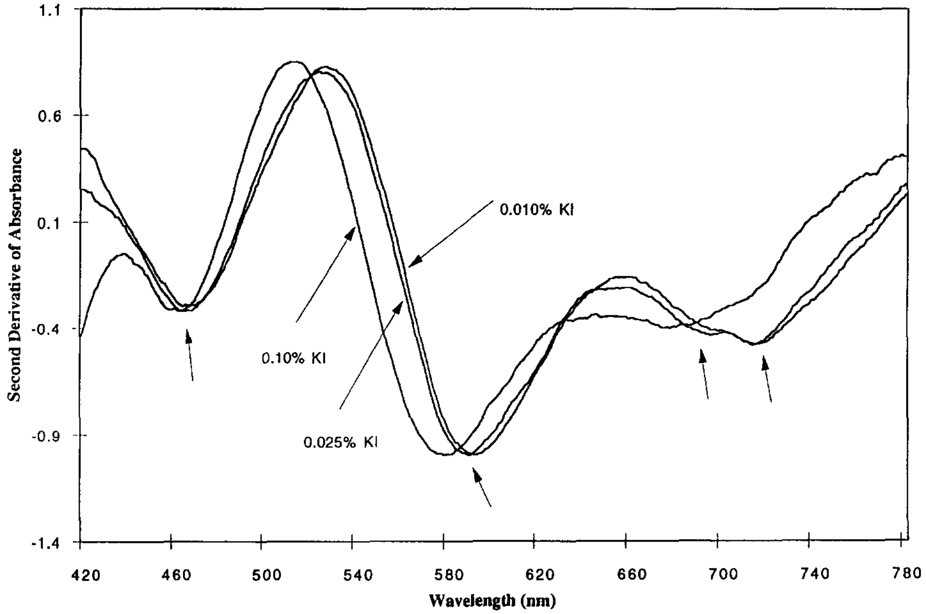

Fig. 4. Second-derivatives of the UV spectra shown in Fig. 3.

iodide concentrations, the peak at 710–740 nm disappears, and the relative intensity of the peak near 660–700 nm declines dramatically, while the intensity of the peak at 560–590 nm increases. Since these bands represent excitation of collective states of the substructures, their interpretation has been undertaken on the basis of the computational analysis.

Computational study of the polyiodide chain.—It was recognized very early [9] that the polyiodide chain may be amenable to a simplified theoretical treatment. One may be able to use the polyene methods popularized by Kuhn [10] to describe the electronic excitations responsible for the observed UV/vis spectra. Fortunately, simple molecular systems such as the polyiodide chain can also be easily studied using semiempirical methods. Since there are a large number of structural variables that will have a significant effect on the results, a more sophisticated approach, such as *ab initio*, is neither warranted nor necessary for the present purpose. With the addition of multielectron configuration interaction (MECI) methods to MOPAC 6.0, it can now be used to estimate the energies and transition moments of electronic excitations. For the purposes of the present work, a very simple model was used. The iodide chain was assumed to be linear with an interatomic distance of 3.1 Å. To determine the overall charge, all chains were assumed to be composed of triiodide or pentaiodide molecules. For example I_{11} was assumed to have a charge of -3, since it could be composed of two triiodide molecules and one pentaiodide. Clearly, this is a rather simple model, since it ignores the effect of the polysaccharide, but it is a reasonable starting point for the computational study of polyiodide in the present context. Similar calculations have been previously reported by Minick et al. [17], but they assumed that all the chains had a charge of -1.

Table 1
Maximum absorption positions as calculated by using MOPAC 6.0

Species	Charge	λ_{max} (nm)	Adjusted λ_{max} [a] (nm)	UV/vis peaks (nm)
I_8	−2	477		
I_9	−3	520	480–510	460–480
I_{10}	−2	567		
I_{11}	−3	651	610–640	560–590
I_{12}	−4	683		
I_{13}	−3	729	690–720	660–700
I_{14}	−4	760		
I_{15}	−3	790	730–760	710–740
I_{16}	−4	828		
I_{18}	−4	887		

[a] Adjusted for the estimated affect of the carbohydrate.

The results of the calculations for I_8 to I_{18} were consistent with each other. All of the molecules had a singlet ground state. The first spin-allowed transition had an exactly zero transition moment, and the second spin-allowed transition had a rather large moment. Given the high extinction coefficients of the iodine–starch complexes, it is likely that only transitions that are both spin- and symmetry-allowed should be consid-

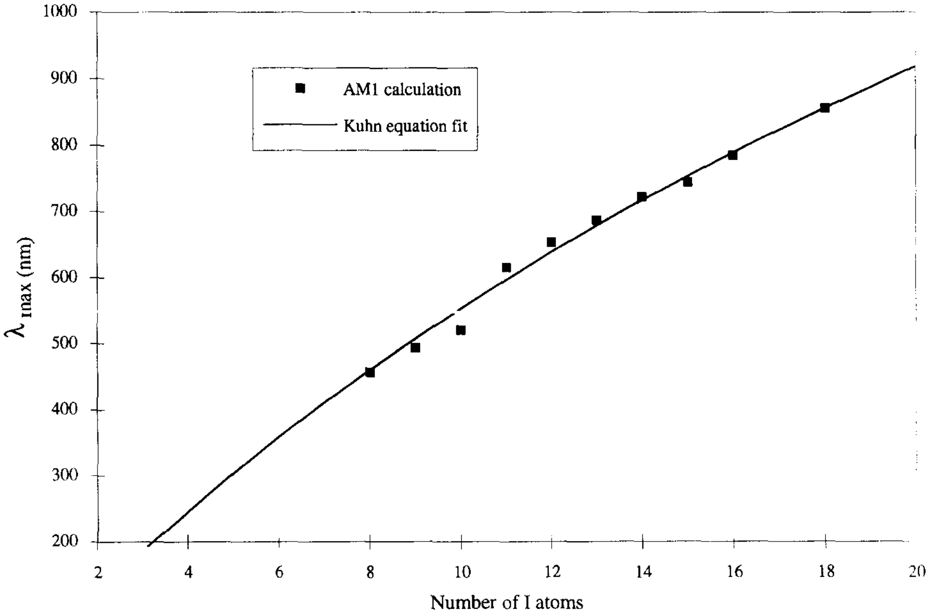

Fig. 5. A plot of the absorption maximum verses iodide chain length. The data for this plot were calculated using MOPAC 6.0. The line is a fit of the Kuhn equation to the calculated data using 0.5 eV as the corrugation height and 4 as the number of electrons contributed by each iodine atom.

ered. Table 1 summarizes the results for the semiempirical calculations using the AM1 Hamiltonian. Only transitions that are both spin- and symmetry-allowed are included in this table, and the UV/vis absorption peaks are also included for comparison.

These data strongly depend on the separation between iodine atoms. For example, when two of the bonds in the I_{11}^{-3} model were changed from 3.1 to 3.0 Å, the first allowed transition shifted to shorter wavelength by 17 nm. Other modifications such as bond angle will also be likely to cause similar effects. Since these calculations assume a vacuum, one must estimate the effect of adding the polysaccharide. The addition of a dielectric medium around the molecules will tend to increase the transition energy by 0.05 to 0.1 eV. Thus one would expect these calculated wavelengths to be approximately 10–40 nm too long, Table 1 includes a column of λ_{max} values adjusted for this effect.

The data shown in Table 1 follow the trend suggested by the Kuhn equation. In the Kuhn equation there are two unknown parameters: the corrugation height and the number of electrons contributed by each atom into the π-system. A least-squares fit of these data results in a value of 0.50 eV for the corrugation height and 4.01 electrons per iodine atom. The data and the fit are shown in Fig. 5.

Comparing the theoretical calculated maximum absorption position, after accounting for the effect of the polysaccharide and the observed UV/vis absorption peaks, one can conclude that four polyiodides, I_9^{3-}, I_{11}^{3-}, I_{13}^{3-}, and I_{15}^{3-}, are the dominant chain lengths in the equilibrium of the polyiodides with iodine and iodide.

3. Discussion

The results of the Raman spectral measurements and those of the UV/vis and theoretical analyses are clearly complementary in that they provide information about structural organization at two different levels. The former points to the occurrence of the I_3^- and I_5^- as the key substructures in the polyiodide chain. The latter indicates that, with respect to the electronic excitations that are responsible for the colors of the complexes, the substructures function cooperatively; all of the dominant absorption bands can be accounted for as collective excitations of three adjacent units of the substructures. The differences between the positions of the absorption maxima appear correlated with the distribution of the population between the two key substructures. Thus, in the most intensely blue complexes, as obtained from saturated iodine solution, without added iodide, it appears that three I_5^- units, taken together, define the electronic excited state. At intermediate levels, first one, then another, and finally all three of the I_5^- units are converted to I_3^- units. The absence of the 180 cm^{-1} band in the Raman spectra clearly rules out participation by I_2 in the polyiodide chain.

With reference to the computational analysis, one can identify the four dominant polyiodide chains as I_9^{3-}, I_{11}^{3-}, I_{13}^{3-}, and I_{15}^{3-}. The dominance of the local modes of I_3^- and I_5^- in the Raman spectra suggests relatively uniform distribution of the electronic charge over the substructural units. The polyiodide chains, as complexes with amylose, exist in an equilibrium with the iodine and iodide in the preparative solution. Thus, changing the concentrations causes changes of their relative populations, which is reflected in shifts in the position of the peaks in the UV/vis spectra. As noted earlier, the peak at around 560–590 nm is always the strongest. If, as seems plausible, it is assumed that the four polyiodide chains have similar extinction coefficients, it would appear that I_{11}^{3-} is the most populated species. This polyiodide chain, however, does not exhibit a blue color, since only a purple color is observed at high iodide concentration, 5% KI. Thus, it is likely that the longer species, I_{13}^{3-} and I_{15}^{3-}, are also present in significant amounts when blue complexes are formed.

Our interpretation is consistent with previous studies. For example, the observations that amylose with a dp of 40–50 can form a blue amylose–iodine complex [2,11,12], which have been noted above, point to a polyiodide chain shorter than 20, when the structure of the amylose helix is taken into account. It has also been observed that amylose with a dp of 30 or less results in complexes that are purple or red, rather than blue. Assuming that the amylose adopts the same helical structure, the observation points to a polyiodide chain of 12 or fewer atoms. Thus our interpretation is consistent with the observed amylose chain length requirements.

Our interpretation is also consistent with the results of studies of potentiometric titrations, which provide the most reliable data for the I_2/I^- ratio. Gilbert and Marriot [13] have reported this ratio as 1.52 for a complex formed in a solution that is 10^{-4} M in iodide and 2.84×10^{-6} M in iodine. When the iodide concentration is increased, the ratio shifts to 1.38. They also observed that this ratio decreases with increasing iodide concentration. For polyiodide chains I_9^{3-}, I_{11}^{3-}, I_{13}^{3-}, and I_{15}^{3-}, their I_2/I^- ratio are respectively 1, 1.33, 1.67, and 2. Clearly, increasing the iodide concentration would tend to favor the shorter chain lengths and shift the ratio to lower values.

With respect to the initial motivation for this work, to which we alluded in the introduction, our findings suggest that the key to understanding the distinctive colors elicited by the different types of fibers when the iodide stains are applied, must be related to the manner in which the substrates influence the coupling of the substructures of the polyiodide chains. Thus, the present study has indeed provided us with a foundation for further studies of the action of iodine/iodide-based stains on cellulosic fibers and the related cell-wall polysaccharides.

4. Experimental

Materials.—Potato amylose was purchased from Sigma Chemical Co. The solution was prepared by first dissolving 0.05 g of amylose in 2 mL of 0.1 N NaOH. This solution was then diluted to about 70–80 mL, neutralized with 2 mL of 0.1 N HCl and diluted to 100 mL. Iodine was a commercial reagent-grade product and used without further treatment.

Raman spectroscopy.—The amylose–iodine complex from saturated iodine and without added iodide solution was prepared by immersing a small dialysis bag containing solid iodine in a 0.05% amylose solution; the iodine can diffuse through the wall of the bag and form a complex with the amylose in the solution. After a few of days, a dark blue precipitate formed. This solid was separated by centrifugation and washed with saturated iodine solution (without added iodide).

Amylose–iodine complexes formed from solutions of 1% and 10% iodide were prepared by adding 0.05 g of iodine to 100 mL of the appropriate iodide solution containing 0.05% amylose. After 1 h of stirring, the precipitate was separated by centrifugation and washed with the appropriate iodide solution. Samples were placed in 5 mm NMR tubes. The Raman spectra were recorded with Nd:YAG (1064 nm) laser excitation using a Bruker RFS 100 FT Raman system.

UV/vis spectroscopy.—The solutions for recording UV/vis spectra contained 0.01% amylose and 10^{-5} M iodine with the iodide concentration varying from 0.010% to 10%. The reference solutions contained the same iodine and iodide concentrations, but with no amylose; they showed no visible absorption between 400 and 900 nm. The UV/vis spectra were acquired using a Perkin–Elmer Lambda 6 spectrophotometer and were converted to second-derivative spectra with a software utility supplied by the manufacturer. The parameters used for the differentiation were width factor 6 and number of points 37.

MOPAC 6.0 calculations.—The semiempirical calculations were performed using the AMPAC/MOPAC module of Insight II 2.30 distributed by Biosym Technologies, Inc. The spin restricted AM1 Hamiltonian was used for all the calculations. Five molecular orbitals were used in the multielectron configuration interaction calculation. A single point calculation for the I_{11}^{-3} model required 1.3 s on and SGI XS24 R4000 workstation. The transition moments were estimated from the orbital mixing matrix found in the detailed summary of the MECI results.

Acknowledgements

This work has been supported in part by the USDA Forest Service and by a Grant from the Division of Energy Biosciences of the Office of Basic Energy Sciences of the US Department of Energy.

References

[1] I.H. Isenberg, *Pulp and Paper Microscopy*, 3rd ed., The Institute of Paper Chemistry, Appleton, Wisconsin, 1967, pp 224–234.

[2] J. Hollo and J. Szeitli, *The Reaction of Starch with Iodine*, in J.A. Radley (Ed.), *Starch and its Derivatives*, 4th ed., 1968, Chapman and Hall Ltd., pp 203–246.

[3] R.E. Rundle and R. Baldwin, *J. Am. Chem. Soc.*, 65 (1943) 544–557.

[4] R.E. Rundle and D. French, *J. Am. Chem. Soc.*, 65 (1943) 558–561.

[5] R.E. Rundle and D. French, *J. Am. Chem. Soc.*, 65 (1943) 1707–1710.

[6] R.E. Rundle and F.C. Edwards, *J. Am. Chem. Soc.*, 65 (1943) 2200–2203.

[7] R.E. Rundle, J.F. Foster, and R. Baldwin, *J. Am. Chem. Soc.*, 66 (1944) 2116–2120.

[8] R.E. Rundle, *J. Am. Chem. Soc.*, 69 (1947) 1769–1772.

[9] S. Ono, S. Tsuchihashi, and S. Kuge, *J. Am. Chem. Soc.*, 75 (1953) 3601–3602.

[10] H. Khun, *J. Chem. Phys.*, 17 (1949) 1198–1212.

[11] D.L. Mould, *Biochem. J.*, 58 (1954) 593–600.

[12] W. Jarowenko, *Starch*, in H.F. Mark, N.G. Gaylord, and N.M. Bikales (Eds.), *Encyclopedia of Polymer Science and Technology*, Vol. 12, Interscience Publishers, 1970, pp 807–808.

[13] G.A. Gilbert and J.V.R. Marriot, *Trans. Faraday Soc.*, 44 (1948) 84–93.

[14] A. Cesaro and W. Konic, *ACS Symp. Ser.*, 150 (1980) 477–490.
[15] T. Handa and H. Yajima, *Biopolymers*, 19 (1980) 1723–1741.
[16] H. Murakami, *J. Chem. Phys.*, 22(3) (1954) 367–374.
[17] M. Minick, K. Fotta, and A. Khan, *Biopolymers*, 31 (1991) 57–63.
[18] T. Watanabe, K. Ogawa, and S. Ono, *Bull. Chem. Soc. Jpn.*, 43 (1970) 950.
[19] F. Cramer and W. Herbst, *Naturwissenschaften*, 39 (1952) 256–258.
[20] K. Freudenberg, E. Schaaf, G. Dumpert, and T. Ploetz, *Naturwissenschaften*, 22 (1939) 850–853.
[21] J.N. Liang, C.J. Knaus, and R.R. Meyers, *Rheol. Acta*, 13 (1974) 740–744.
[22] R.C. Teitelbaum, S.L. Ruby, and T.J. Marks, *J. Am. Chem. Soc.*, 102 (1980) 3322–3328.
[23] J.A. Thoma and D. French, *J. Am. Chem. Soc.*, 82 (1960) 4144–4147.
[24] J.M. Reddy, K. Knox, and M.B. Robin, *J. Chem. Phys.*, 40 (1964) 1082–1089.
[25] M.B. Robin, *J. Chem. Phys.*, 40 (1964) 3369–3377.
[26] T. Handa and H. Yajima, *Biopolymers*, 18 (1979) 873–886.
[27] M. Noltemeyer and W. Saenger, *J. Am. Chem. Soc.*, 102 (1980) 2710–2722.
[28] B. Pfannemüller and G. Ziegast, *ACS Symp. Ser.*, 150 (1980) 529–547.
[29] G. Ziegast and B. Pfannemüller, *Int. J. Biol. Macromol.*, 4 (1982) 419–424.
[30] A.G. Maki and R. Fourneris, *Spectrochim. Acta A*, 23 (1967) 867–880.
[31] F.W. Parrett and N.J. Taylor, *J. Inorg. Nucl. Chem.*, 32 (1970) 2458–2461.
[32] E.M. Nour, L.H. Chen, and J. Laane, *J. Phys. Chem.*, 90 (1986) 2841–2846.
[33] H. Mittag, H. Stegemann, and H. Fuller, *J. Raman Spectrosc.*, 20 (1989) 251–255.
[34] M. Mizuno and J. Tanaka, *J. Phys. Chem.*, 85 (1981) 1789–1794.
[35] K. Murdoch, *Carbohydr. Res.*, 233 (1992) 161–174.
[36] J.F. Cahill, *Am. Lab.*, 11(11) (1979) 79–85.
[37] J.F. Cahill and F.G. Padera, *Am. Lab.*, 12(4) (1980) 101–112.